Paper No.
05057

CORROSION2005

A Stochastic Prediction Model of Localized CO_2 Corrosion

Ying Xiao and Srdjan Nešić

Institute for Corrosion and Multiphase Technology
342West State Street, Ohio University, Athens, OH 45701

ABSTRACT

In this paper a two-dimensional (2-D) stochastic localized CO_2 corrosion model is proposed, which describes the balance of two processes: corrosion (leading to metal loss) and precipitation (leading to metal protection). The model is able to predict localized corrosion of carbon steel in CO_2 containing environments.

The model uses corrosion rate and surface-scaling tendency predicted by a 1-D mechanistic corrosion model as the inputs. It can predict the possibility of localized corrosion as a function of primitive parameters such as temperature, pH, partial pressure of CO_2, velocity, etc. The maximum pit penetration rate as well as the uniform corrosion rate can be predicted and used to describe the severity of the localized attack.

Keywords: localized corrosion, model, stochastic, pitting, iron carbonate, scaling tendency, carbon steel

INTRODUCTION

In order to operate the oil and gas pipelines under safe and reliable conditions, it is important to predict the internal corrosion that occurs in a CO_2 containing environment. In practice, localized corrosion is the most serous and frequent cause of pipeline failure. Therefore, it is necessary to predict the occurrence of localized CO_2 corrosion of carbon and low alloy steels materials.

While uniform CO_2 corrosion of carbon steel has received much attention far fewer studies focused on localized attack. Nyborg[1] investigated initiation and growth of mesa attack in flow loop experiments. He proposed that a partially protective corrosion film is a prerequisite for mesa attack. Schmitt[2, 3] developed a probabilistic model for the prediction of flow induced localized corrosion. This approach is promising however it is well established that besides the flow a number of other environmental factors such as solution chemistry, temperature, pressure, and pH value, etc., can affect

the localized CO_2 corrosion rate of mild steel.[4] Therefore, a successful model that could predict the localized attack must takes all of these into account.

Brossia[5] studied a number of parameters that influence localized attack. He could not identify a clear dependency of the severity or mode of attack on each independent parameter and the initiation of pitting seemed to be of stochastic (random) nature. The probabilistic characters of localized attack makes a stochastic approach to its study attractive[6, 7, 8].

Sun and Nesic[9] studied a number of factors that might influence localized corrosion in wet gas flow, including pH, temperature, pressure, flow velocity, flow regime, water cut and steel type. These studies confirmed Nyborg's assumption that partially protective film is a prerequisite for localized attack.

In 1996, van Hunnik and Pots[10] have reported a development of a 2-D stochastic algorithm program to simulate the morphology of localized attack. The algorithm resides on the assumption that the morphology of corrosion attack depends on the balance of two processes: corrosion (leading to metal loss) and precipitation (leading to metal protection). This balance has effectively been quantified by van Hunnik and Pots[10] using a single parameter: the scaling tendency (ST):

$$ST = \frac{R_{FeCO_3}}{CR} \tag{1}$$

where R_{FeCO_3} is the precipitation rate of iron carbonate and CR the corrosion rate, both expressed in the same volumetric units (e.g. mm/y). It has been experimentally observed that if the precipitation rate overwhelms the corrosion rate, a protective film forms at the metal surface and the corrosion rate is greatly reduced. On the other hand, if the corrosion rate is much larger than the precipitation rate, protective films cannot form as corrosion creates voids underneath the film faster than precipitation can fill them up. According to a recent experimental study by Sun and Nesic[4], there is a "gray zone" between these extremes where localized corrosion occurs.

Given the same ST value, the van Hunnik and Pots[10] algorithm leads to somewhat different surface morphologies every time the simulation is repeated. Nevertheless, the overall nature of the attack remains the same as illustrated in a follow-up paper by Nesic et al.[11] on the developments of the stochastic localized corrosion model. There it was shown how the original van Hunnik and Pots[10] algorithm was improved and linked to the 1-D mechanistic model of CO_2 corrosion[12,13,14]. This linkage enabled prediction of the scaling tendency ST based on the input of primitive variables such as temperature, velocity, CO_2 partial pressure, pH etc. It was shown that the algorithm captures the experimental behavior reported by Sun and Nesic[4] related to localized corrosion occurring in the "grey zone" when partially protective films form. There it was argued that in order to be able to predict localized attack, it was sufficient to assume a partially protective film and stochastic nature of the corrosion and precipitation processes.

NEW MODEL DEVELOPMENTS

Following the initial breakthrough developments[10,11] further improvements and adjustments of the stochastic localized corrosion model is reported below.

It is well known that to initiate precipitation, the solution must be supersaturated. The precipitation takes place in two stages: nucleation and growth[15]. Both processes are related to the level of supersaturation. At a high supersaturation, iron carbonate crystals may rapidly nucleate in a large number of locations and grow fast to form a thin tight surface film with small crystal size. These films are usually very protective. At a low supersaturation, nucleation happens in a significantly smaller number of locations, the crystal growth proceeds slowly and the crystals become very large. Furthermore, the large crystals form a much thicker and looser surface layer that is less protective and is easier damaged or swept away by the flow. Both the nucleation and crystal growth have been implemented into the new version of the model. To account for the effect of nucleation, a "quadratic time-delay" factor has been added to the precipitation rule in the algorithm. For more details see the original work by Xiao[16].

A film growth algorithm was also implemented to make the whole localized attack simulation appear and perform more realistically. The film in the simulation grows proportionally to the precipitation rate which is predicted by the mechanistic 1-D model[12,13,14]. The algorithm of iron carbonate film growth was implemented initially by assuming that the newly precipitated film deposits directly on top of any previous film. Figure 1 shows the typical film morphology obtained in simulation studies by using this algorithm. In this figure, a clear solution layer, a porous film layer, a dense film layer, and the detached layer between film and metal can be easily observed. However, the structure of the film does not seem realistic in Figure 1, the tower-like structures do not resemble typical iron carbonate film morphology. In an experimental study Joosten et al. [17] found that iron carbonate crystals that form on carbon steel have self-similar structural properties not unlike fractals. In the latest version of the new model, this has been implemented by allowing the newly formed layers of iron carbonate film to precipitate in any direction randomly. The film structure formed in this way is more porous than the previous one and takes on a more realistic appearance (shown in Figure 2 and as a close-up in Figure 3). Furthermore, in Figure 4, we can see that with this modification the shape of the pits that are predicted during localized attack becomes more rounded.

A pitting factor can be used Jones[18] to quantify the severity of pitting:

$$f = \frac{PR}{CR} \tag{2}$$

where, f is the pitting factor, PR is the maximum pitting penetration rate in mm/yr and CR is the uniform corrosion rate in mm/yr. A pitting factor of unity indicates uniform corrosion. The higher the pitting factor is the higher severity of localized corrosion. It is judged that when the pitting factor is 3 or above, this indicates that severe localized corrosion occurs.

RESULTS

Comparisons

The present 2-D model has been successfully linked with the 1-D mechanistic model[12,13,14] that can predict the uniform corrosion rate for different pH, temperature, partial pressure of CO_2, water chemistry, flow velocity, flow regime, etc. Comparison of the present stochastic localized 2-D model

predictions, which include prediction of uniform corrosion (CR) and localized pitting penetration rate (PR), with 1-D uniform corrosion predictions and selected LPR experimental results[19] is shown in Figure 5, Figure 6, and Figure 7. Since the inputs of the present 2-D model are the initial corrosion rate and surface scaling tendency predicted by the 1-D model, it is not surprising that the corrosion predicted by 2-D simulation agrees with the result from 1-D prediction, at the beginning of the simulation. However, the agreement of the film growth process and its ultimate protectiveness are independent and done differently in the 1-D and 2-D models. The good agreement seen demonstrates that the 2-D stochastic model performs reasonably well in predicting the uniform corrosion in the presence of protective films (or just as good as the 1-D model). What is more important, the 2-D model can predict localized attack by calculating pitting factor while the 1-D model cannot.

Parametric study

To demonstrate the capabilities of the 2-D model, a variety of simulations is presented below leading to a range of different surface morphologies and corrosion rates In Figure 8 - Figure 14. In Figure 8, we see that when there is no Fe^{2+} in the solution, there is no iron carbonate film formed under the conditions specified. The corrosion rate does not change with time and uniform attack (2.6 mm/y) is obtained with a unity pitting factor. This can be deduced by looking at the magnitude of the uniform corrosion rate (CR) and the maximum penetration rate (PR) which is similar. At Fe^{2+}=5 ppm there is some precipitation and a porous unprotective film forms comprised of large crystals (Figure 9). The corrosion rate deceases slowly and the final corrosion is lower than in the first case. The pitting factor of 1.1 suggests uniform attack. As the Fe^{2+} concentration is increased to 10 ppm (see Figure 10) and 25 ppm (see Figure 11) more film precipitates and the corrosion rate decreases more rapidly to a steady state value of 1.3 and 1.1 mm/y respectively. The film is still rather porous with smaller grain size, still not really protective. There is no localized attack (CR≈PR) with pitting factor of 1.1 and 1.3 respectively. Further increase of Fe^{2+} concentration to 28 ppm leads to even more and denser film formation (Figure 12). However, it takes the overall conditions into the "grey zone" and localized attack is initiated just as Sun[20] has observed in experiments. The maximum rate of localized attack seen is approximately 0.6 mm/y while the uniform corrosion proceeds at about 0.1 mm/y. This leads to a high pitting factor of 5.9. Further increase in Fe^{2+} concentration to 30 ppm (Figure 13) also results initially in localized attack with a pitting factor of 3.7. However, most of the pits heal and both the uniform and localized rates of attack are lower than in the previous case. Finally, 50 ppm of Fe^{2+} results in stable formation of protective films with very little corrosion (Figure 14). The pitting factor of 4.4 is still rather high; however the magnitude of localized corrosion is not so worrisome with the maximum penetration rate of 0.15 mm/y.

This parametric study is shown only as an example of the variety of corrosion attack outcomes that can be predicted by the newly developed model. Indeed there are numerous other parameter combinations that lead to localized attack and their presentation exceeds the scope of this paper.

CONCLUSIONS

The newly developed stochastic 2-D model is capable of predicting localized CO_2 corrosion morphologies found in practice. The new nucleation algorithm and film growth assist in predicting more realistic film morphology and corrosion rate.

The model which can predict localized corrosion as a function of primitive parameters such as temperature, pH, partial pressure of CO_2, velocity, has been successfully calibrated at different film precipitation conditions.

ACKNOWLEDGEMENT

The author would like to sincerely thank Dr. Bert. M. Pots for sharing his original ideas that got this project going and his suggestions on how to improve this work. The author would like to acknowledge the companies who sponsor this work, they are BP, Champion, Clariant, ConocoPhilips, ExxonMobil, MI, Nalco, Saudi Aramco, Shell, and Total.

REFERENCES

1. R. Nyborg, "Intiation and Growth of Mesa Corrosion Attack during CO_2 Corrosion of Carbon Steel," CORROSION/1998, Paper No. 48, NACE International, Houston, Texas, 1998.
2. G. Schmitt, T. Gudde, and E. Strobel-Effertz, "Fracture Mechanical Properties of CO_2 Corrosion Product Scales and their Relation to Localized Corrosion," CORROSION/1996, Paper No. 9, NACE International, Houston, Texas, 1996.
3. G. Schmitt, C. Bosch, M. Mueller, G. Siegmund, "A Probabilistic Model for Flow Induced Localized Corrosion," CORROSION/2000, Paper No. 49, NACE International, Houston, Texas, 2000.
4. Y. Sun, K. George, S. Nesic, "A Parametric Study And Modeling On Localized Co2 Corrosion In Horizontal Wet Gas Flow", CORROSION/2003, Paper No. 3327, NACE International, Houston, Texas, 2003.
5. C.S. Brossia, and G.A. Cragnolino, "Effect of Environmental Variables on Localized Corrosion of Carbon Steel," Corrosion, 56, 505-514, 2000.
6. D. E. Williams, C. Westcott, M. Fleischmann, J. Electroanal. Chem., 1984, 180, 549.
7. D. E. Williams, C. Westcott, and M. Fleischmann, J. Electrochem. Soc., 1985, 132, 1796.
8. U. Bertocci, F. Huet, Corrosion, 1995, 51, 131.
9. Y. Sun, Dissertation, Institute of Corrosion and Multiphase Technologies, 2003.
10. E.W.J. van Hunnik, B.F.M. Pots, CORROSION/1996, Paper No. 6.
11. S. Nesic, Y. Xiao, and B.F.M. Pots, "A Quasi 2-D localized Corrosion Prediction Model," CORROSION/2004, Paper No. 04628, NACE International, Houston, Texas, 2004.
12. M. Nordsveen, S. Nesic, R. Nyborg, and A. Stangeland, "A Mechanistic Model for Carbon Dioxide Corrosion of Mild Steel in the Presence of Protective Iron Carbonate Films-Part 1: Theory and Verification", Corrosion, 2003, 59,443.
13. S. Nesic, K. J. Lee, Corrosion, 2003, 59,616.
14. S. Nesic, M. Nordsveen, R. Nyborg, A. Stangeland, Corrosion, 2003, 59,489.
15. Ph. Calarch, "Theoretical Introduction to Precipitation's Phenomena", published online: 7 Mar 2001, at http://www.nano-tek.org/main.html
16. Y. Xiao, "A Study on Stochastic Modeling of Localized Corrosion", Ohio University Thesis, Nov. 2004.
17 M.W. Joosten, T. Johnsen, H. H. Hardy, T. Jossang, and J. Feder, "Fractal Behavior of CO2 Pits", Corrosion/92, Paper No. 11, NACE International, Houston, Texas, 1992.
18. Jones, D.A, Principles and Prevention of Corrosion, 2nd edition, Englewood Cliffs, NJ : Prentice Hall ; London : Prentice-Hall International, 1996.
19. K. Chokshi, Institute for Corrosion and Multiphase Technology, Ohio Unversity, Board Meeting Report, Sep, 2003.
20. Y. Sun, "Localized CO_2 Corrosion In Horizontal Wet Gas Flow", Ohio University Dissertation, Mar. 2003.

TABLES AND FIGURES

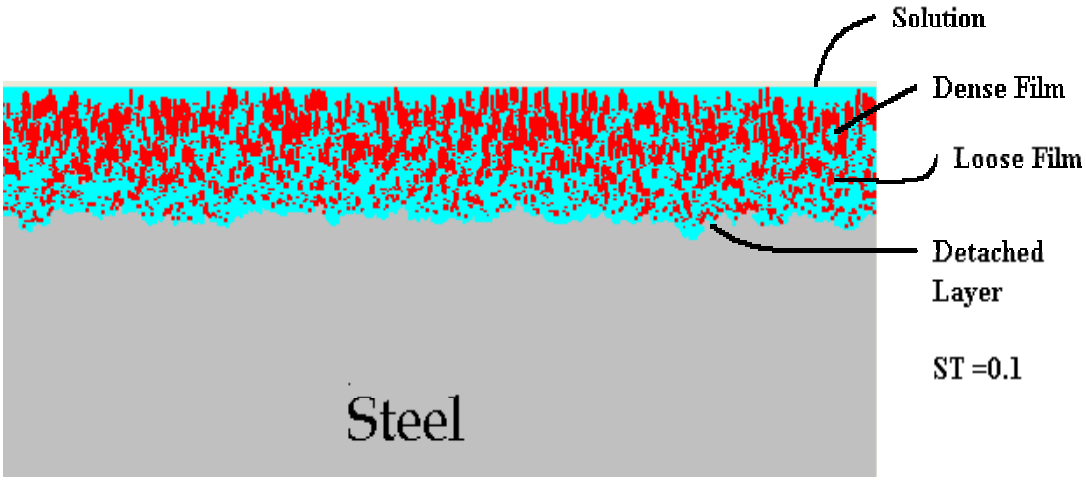

Figure 1. Film morphology taken from the proposed 2-D Model.

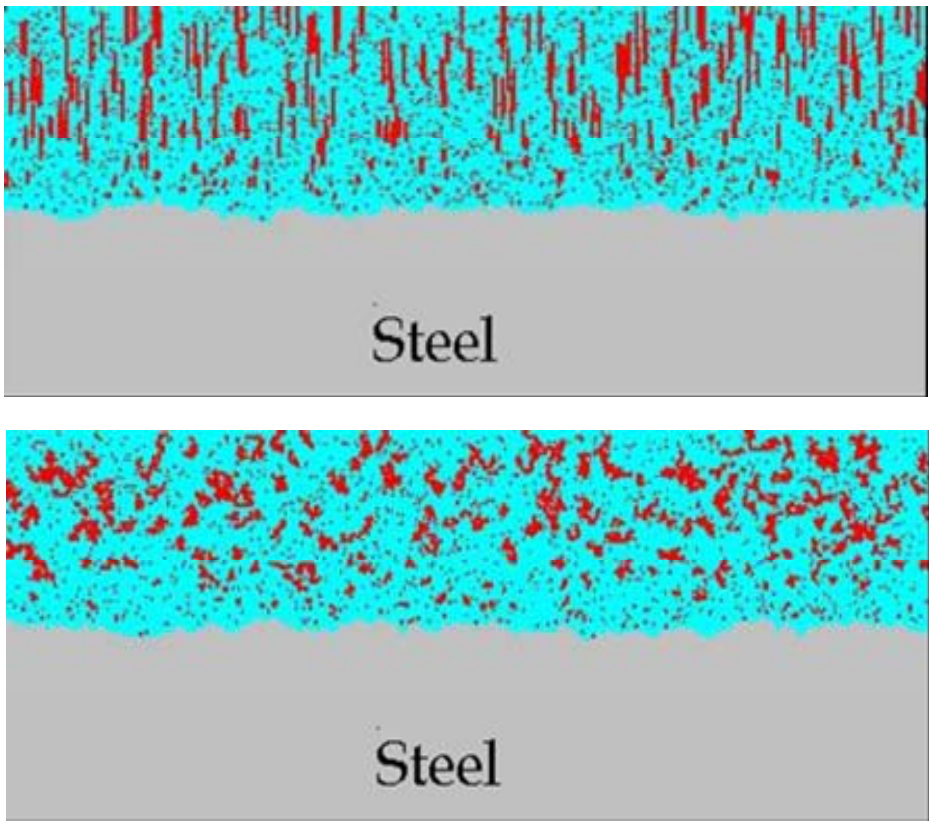

Figure 2. Comparison of the film morphology before (top) and after (bottom) using a random film formation algorithm at pH 6.6, 80°C, 5ppm Fe^{2+} and 0.52bar p_{CO2}.

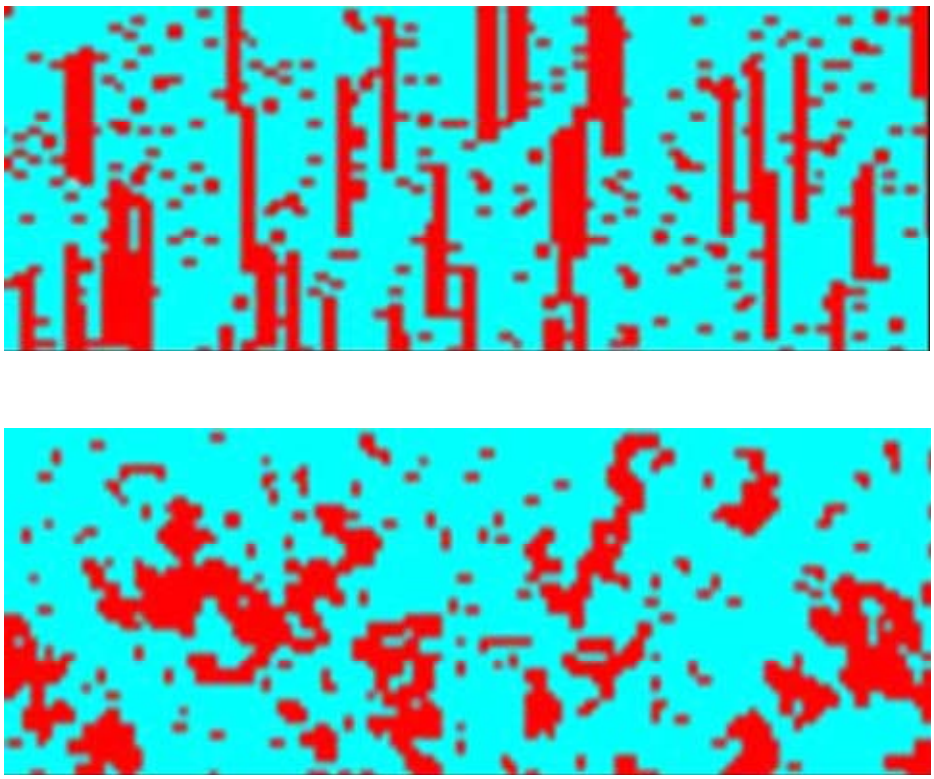

Figure 3. Comparison of the film morphology at higher magnification before (top) and after (bottom) using a random film formation algorithm at pH 6.6, 80°C, 5ppm Fe^{2+} and 0.52bar p_{CO2}.

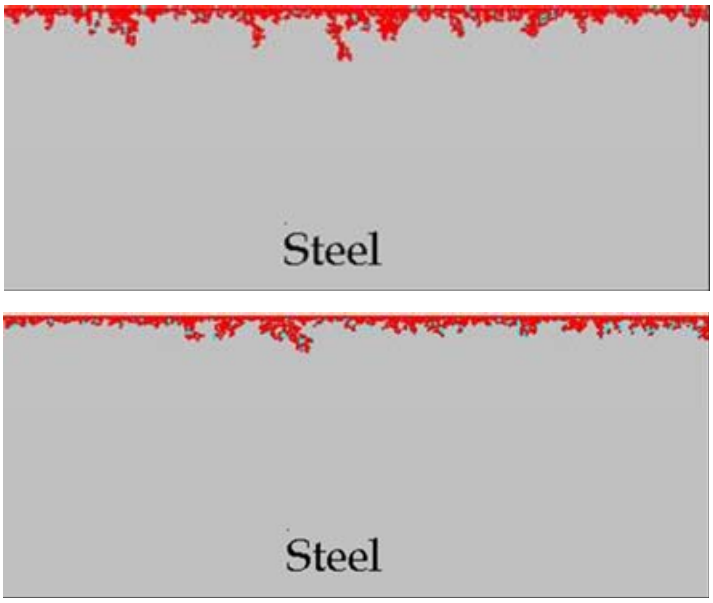

Figure 4. Comparison of the film morphology before (top) and after (bottom) using a random film formation algorithm at pH 6.5, 80°C, 50ppm Fe^{2+} and 0.52bar p_{CO2}.

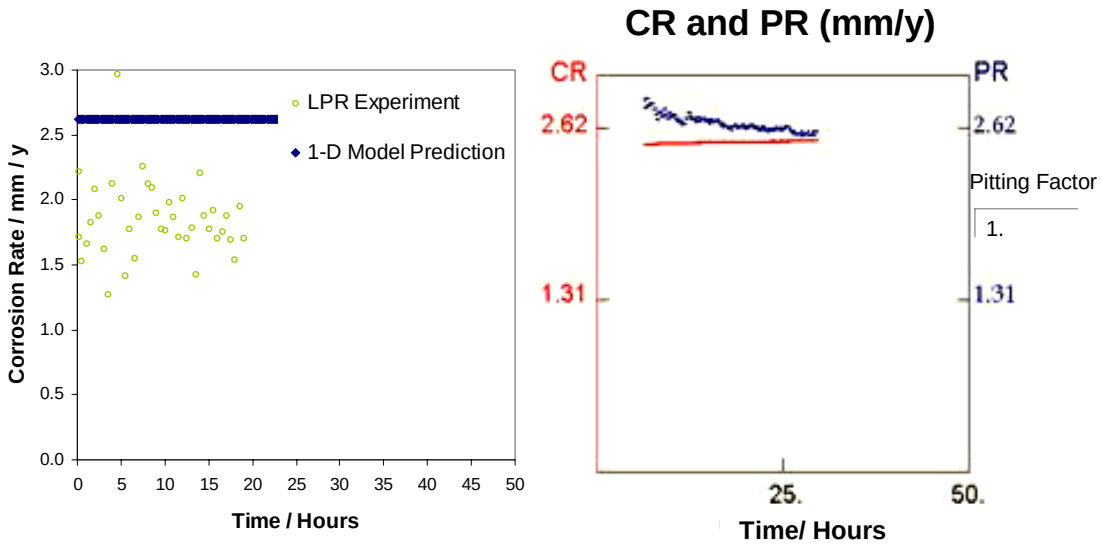

Figure 5. Comparison of corrosion rate obtained from 1-D prediction model[12,13,14], LPR experimental data[19] (shown on the graph on the left) and the present 2-D prediction (shown on the graph on the right) including prediction of uniform corrosion (lower line denoted CR), localized pit penetration rate (upper curve denoted PR) and pitting factor (f=1). Conditions: pH 6.0, 80°C, 0.52bar P_{CO2}, 50ppm Fe^{2+}, and stagnant.

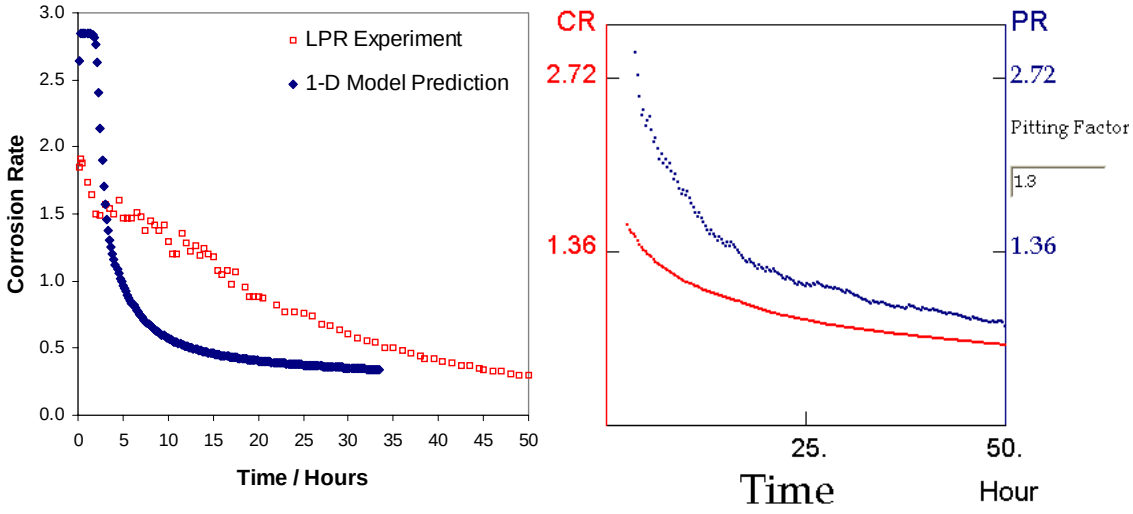

Figure 6. Comparison of corrosion rate obtained from 1-D prediction model[12,13,14], LPR experimental data[19] (shown on the graph on the left) and the present 2-D prediction (shown on the graph on the right) including prediction of uniform corrosion (lower curve denoted CR), localized pit penetration rate (upper curve denoted PR) and pitting factor (f=1.3). Conditions: pH 6.3, 80°C, 0.52bar P_{CO2}, 50ppm Fe^{2+}, and stagnant.

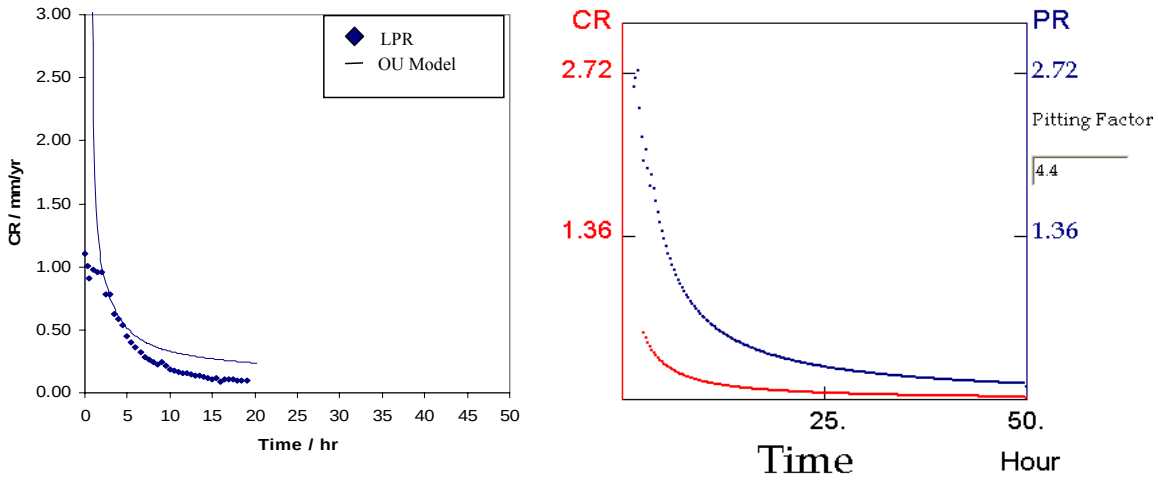

Figure 7. Comparison of corrosion rate obtained from 1-D prediction model[12,13,14], LPR experimental data[19] (shown on the graph on the left) and the present 2-D prediction (shown on the graph on the right) including prediction of uniform corrosion (lower curve denoted CR), localized pit penetration rate (upper curve denoted PR) and pitting factor (f=4.4). Conditions: pH 6.6, 80°C, 0.52bar P_{CO2}, 50ppm Fe^{2+}, and stagnant.

Figure 8. Surface morphology and the trend of the corresponding uniform corrosion rate (lower curve denoted CR) and localized penetration rate (upper curve denoted PR) as predicted by 2-D model at 0 ppm Fe^{2+}, 0.54bar pCO_2, 80 °C, pH 6.6, and 1m/s.

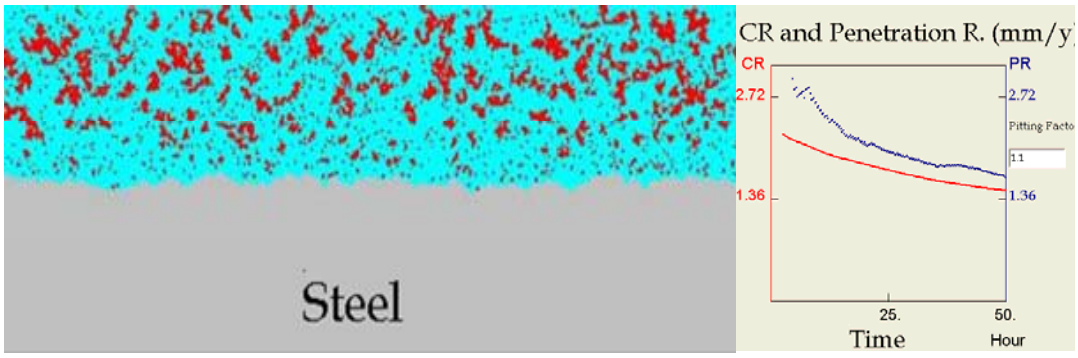

Figure 9. Surface morphology and the trend of the corresponding uniform corrosion rate (lower curve denoted CR) and localized penetration rate (upper curve denoted PR) as predicted by 2-D model at 5 ppm Fe^{2+}, 0.54bar pCO_2, 80 °C, pH 6.6, and 1m/s.

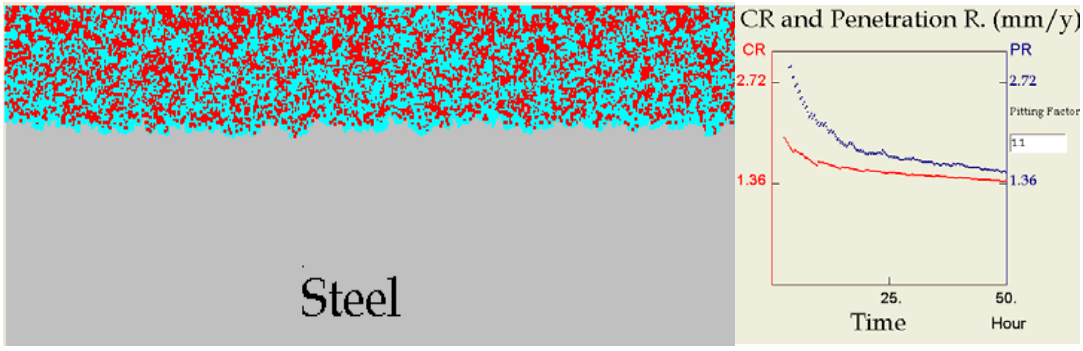

Figure 10. . Surface morphology and the trend of the corresponding uniform corrosion rate (lower curve denoted CR) and localized penetration rate (upper curve denoted PR) as predicted by 2-D model at 10 ppm Fe^{2+}, 0.54bar pCO_2, 80 °C, pH 6.6, and 1m/s.

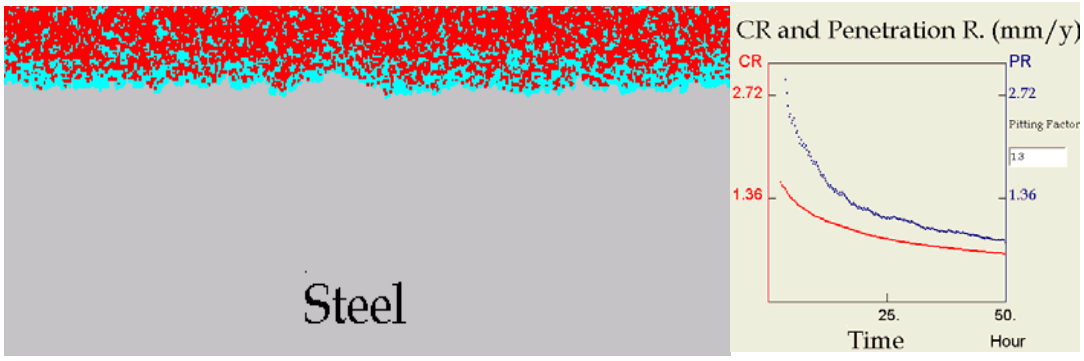

Figure 11. . Surface morphology and the trend of the corresponding uniform corrosion rate (lower curve denoted CR) and localized penetration rate (upper curve denoted PR) as predicted by 2-D model at 25 ppm Fe^{2}, 0.54bar pCO_2, $^{+}$, 80 °C, pH 6.6, and 1m/s.

Figure 12. Surface morphology and the trend of the corresponding uniform corrosion rate (lower curve denoted CR) and localized penetration rate (upper curve denoted PR) as predicted by 2-D model at 28 ppm Fe^{2+}, 0.54bar pCO_2, 80 °C, pH 6.6, and 1m/s.

Figure 13. Surface morphology and the trend of the corresponding uniform corrosion rate (lower curve denoted CR) and localized penetration rate (upper curve denoted PR) as predicted by 2-D model at 30 ppm Fe^{2+}, 0.54bar pCO_2, 80 °C, pH 6.6, and 1m/s.

Figure 14. Surface morphology and the trend of the corresponding uniform corrosion rate (lower curve denoted CR) and localized penetration rate (upper curve denoted PR) as predicted by 2-D model at 50 ppm Fe^{2+}, 0.54bar pCO_2, 80 °C, pH 6.6, and 1m/s.